

THE RELATION BETWEEN BLACK HOLE MASS, BULGE MASS, AND NEAR-INFRARED LUMINOSITY

ALESSANDRO MARCONI¹ AND LESLIE K. HUNT²
Astrophysical Journal Letters, in press

ABSTRACT

We present new accurate near-infrared (NIR) spheroid (bulge) structural parameters obtained by two-dimensional image analysis for all galaxies with a direct black hole (BH) mass determination. As expected, NIR bulge luminosities L_{bul} and BH masses are tightly correlated, and if we consider only those galaxies with secure BH mass measurement and accurate L_{bul} (27 objects), the spread of $M_{\text{BH}}-L_{\text{bul}}$ is similar to $M_{\text{BH}}-\sigma_e$, where σ_e is the effective stellar velocity dispersion. We find an intrinsic *rms* scatter of $\simeq 0.3$ dex in $\log M_{\text{BH}}$. By combining the bulge effective radii R_e measured in our analysis with σ_e , we find a tight linear correlation (*rms* $\simeq 0.25$ dex) between M_{BH} and the virial bulge mass ($\propto R_e \sigma_e^2$), with $\langle M_{\text{BH}}/M_{\text{bul}} \rangle \sim 0.002$. A partial correlation analysis shows that M_{BH} depends on both σ_e and R_e , and that both variables are necessary to drive the correlations between M_{BH} and other bulge properties.

Subject headings: black hole physics – galaxies: bulges – galaxies: nuclei – galaxies: fundamental parameters

1. INTRODUCTION

Central massive black holes (BHs) are now thought to reside in virtually all galaxies with a hot spheroidal stellar component (hereafter bulge). Such BHs seem to be a relic of past quasar activity (e.g., Sothman 1982; Marconi & Salvati 2002; Yu & Tremaine 2002; Aller & Richstone 2002) and related to host galaxy properties, with the implication that BH and galaxy formation processes are closely linked. Previous work has shown that BH mass M_{BH} is correlated with both blue luminosity $L_{\text{B,bul}}$ and bulge mass M_{bul} , although with considerable intrinsic scatter (*rms* ~ 0.5 in $\log M_{\text{BH}}$; Kormendy & Richstone 1995). However, M_{BH} and the bulge effective stellar velocity dispersion σ_e correlate more tightly (*rms* ~ 0.3) than $M_{\text{BH}}-L_{\text{B,bul}}$ (Ferrarese & Merritt 2000; Gebhardt et al. 2000). The smaller scatter of the $M_{\text{BH}}-\sigma_e$ correlation suggests that the bulge dynamics (or mass), rather than luminosity, is the agent of the correlation. But the smaller spread relative to $M_{\text{BH}}-L_{\text{bul}}$ appears to be an artefact of the manipulations necessary to derive L_{bul} . Indeed, recent work has shown that when bulge parameters are measured with more accuracy [e.g. profile fitting rather than average correction for disk light (Simien & de Vaucouleurs 1986)], the resulting scatter is comparable to that of $M_{\text{BH}}-\sigma_e$ (McLure & Dunlop 2002; Erwin et al. 2003). The correlation between M_{BH} and bulge light concentration also has a comparably low scatter (Graham et al. 2001). Nevertheless, there are strong indications that $L_{\text{B,bul}}$ of the brightest elliptical galaxies, for which decomposition issues are unimportant, deviate significantly from the $M_{\text{BH}}-L_{\text{bul}}$ relation (Ferrarese 2002). Hence, longer wavelengths may also be necessary to better define the intrinsic scatter in $M_{\text{BH}}-L_{\text{bul}}$ compared to that of $M_{\text{BH}}-\sigma_e$.

In this paper, we reexamine the $M_{\text{BH}}-L_{\text{bul}}$ correlation by accurately measuring the bulge luminosity in the near-infrared (NIR) for all galaxies with a well-determined M_{BH} . All previous studies have used optical light (B or R) to test the $M_{\text{BH}}-L_{\text{bul}}$ relation, but NIR light provides a clear advantage over the optical: it is a better tracer of stellar mass and less subject to the effects of extinction. If the physical correlation is between the BH mass and bulge mass, the NIR correlations $M_{\text{BH}}-L_{\text{bul}}$ should be tighter than those in the optical, because of the smaller vari-

ation of M/L ratio Υ with mass (e.g., Gavazzi 1993). Moreover, we use a two-dimensional (2D) bulge/disk decomposition to determine bulge parameters, an improvement on earlier work which applied 1D fits only. Here we construct the largest possible sample, by considering all galaxies which have been used for the $M_{\text{BH}}-\sigma_e$ and $M_{\text{BH}}-L_{\text{B,bul}}$ correlations. In §2 we present the sample of galaxies with direct dynamical BH mass measurements, and in §3 describe the images and the 2D bulge/disk decomposition applied to them. Finally, in §4 we discuss the results of the analysis.

2. THE SAMPLE

To date, there are 37 galaxies with direct gas kinematical or stellar dynamical determination of the central BH mass. These galaxies have been compiled and made into a uniform sample (e.g., for distances) by a number of authors (e.g., Merritt & Ferrarese 2002; Tremaine et al. 2002; hereafter MF02 and T02, respectively). We adopt the data from the recent paper by T02 with some modifications and additions. The data in Columns 1-5 and 9 of Table 1 are from the compilation by T02 and the reader can refer to that paper for more details. Differently from T02, when galaxy distances from surface brightness fluctuations (Tonry et al. 2000) are not available, we use recession velocities corrected for Virgocentric infall from the LEDA database (<http://leda.univ-lyon1.fr/>) with $H_0 = 70 \text{ km s}^{-1} \text{ Mpc}^{-1}$. In a few cases, we also consider BH mass estimates from different papers than those used by T02; thus, in Col. 6, we indicate the appropriate references. With respect to the 31 galaxies considered by T02 we add: Cygnus A (Tadhunter et al. 2003), M81 (Devereux et al. 2003), M84 (Bower et al. 1998), NGC 4594 (Kormendy 1988), Centaurus A (Marconi et al. 2001) and NGC 5252 (Capetti et al. 2003).

Following MF02, we divide the galaxies into two groups. In the first group, we place all the galaxies which have a secure BH mass measurement and an accurate determination of the bulge NIR luminosity. We consider ‘secure’ those BH masses for which the black hole sphere of influence, $R_{\text{BH}} = GM_{\text{BH}}/\sigma_e^2$ (column 7 of Table 1), has been clearly resolved, i.e., $N_{\text{res}} = 2R_{\text{BH}}/R_{\text{res}} > 1$, where R_{res} is the spatial resolution of the obser-

¹ INAF- Osservatorio Astrofisico di Arcetri, L.go Fermi 5, I-50125 Firenze, Italy; marconi@arcetri.astro.it.

² Istituto di Radioastronomia-Sez. Firenze/CNR, L.go Fermi 5, I-50125 Firenze, Italy; hunt@arcetri.astro.it.

TABLE I
 GALAXY SAMPLE.

Galaxy (1)	Type (2)	D (3)	σ_* (4)	$M_{\text{BH}}(+,-)$ (5)	Ref (6)	R_{BH} (7)	N_{res} (8)	M_{B} (9)	M_{J} (10)	M_{H} (11)	M_{K} (12)	R_{e} (13)	M_{bul} (14)
Group 1													
NGC4258	Sbc	7.2	130	$3.9(0.1, 0.1) \times 10^7$	m-1	0.28	71	-17.2	-20.9	-22.0	-22.4	0.92 ± 0.23	$1.1 \pm 0.3 \times 10^{10}$
M87	E0	16.1	375	$3.4(1.0, 1.0) \times 10^9$	g-2	1.33	33	-21.5	-24.6	-25.2	-25.6	6.4 ± 1.6	$6.2 \pm 1.7 \times 10^{11}$
NGC3115	S0	9.7	230	$9.1(9.9, 2.8) \times 10^8$	s-3	1.57	15	-20.2	-23.5	-24.2	-24.4	4.7 ± 1.2	$1.7 \pm 0.5 \times 10^{11}$
NGC4649	E1	16.8	385	$2.0(0.4, 0.6) \times 10^9$	s-4	0.71	14	-21.3	-24.9	-25.5	-25.8	8.1 ± 2.0	$8.4 \pm 2.2 \times 10^{11}$
M81	Sb	3.9	165	$7.6(2.2, 1.1) \times 10^7$	g-5	0.63	13	-18.2	-23.1	-23.9	-24.1	3.4 ± 0.9	$6.4 \pm 1.8 \times 10^{10}$
M84	E1	18.4	296	$1.0(2.0, 0.6) \times 10^9$	g-6	0.55	11	-21.4	-24.7	-25.8	-25.7	8.2 ± 2.1	$5.0 \pm 1.4 \times 10^{11}$
M32	E2	0.8	75	$2.5(0.5, 0.5) \times 10^6$	s-7	0.49	9.7	-15.8	-18.9	-19.7	-19.8	0.24 ± 0.06	$9.6 \pm 2.6 \times 10^8$
CenA	S0	4.2	150	$2.4(3.6, 1.7) \times 10^8$	g-8	2.25	9.0	-20.8	-23.8	-24.3	-24.5	3.6 ± 0.9	$5.6 \pm 1.5 \times 10^{10}$
NGC4697	E4	11.7	177	$1.7(0.2, 0.1) \times 10^8$	s-4	0.41	8.2	-20.2	-23.9	-24.5	-24.6	9.1 ± 2.3	$2.0 \pm 0.5 \times 10^{11}$
IC1459	E3	29.2	340	$1.5(1.0, 1.0) \times 10^9$	s-9	0.39	7.8	-21.4	-24.8	-25.3	-25.9	8.2 ± 2.0	$6.6 \pm 1.8 \times 10^{11}$
NGC5252	S0	96.8	190	$1.0(0.2, 0.4) \times 10^9$	g-10	0.25	5.1	-20.8	-24.4	-25.2	-25.6	9.7 ± 2.4	$2.4 \pm 0.9 \times 10^{11}$
NGC2787	SB0	7.5	140	$4.1(0.4, 0.5) \times 10^7$	g-11	0.25	5.0	-17.3	-20.4	-21.1	-21.3	0.32 ± 0.08	$4.4 \pm 1.2 \times 10^9$
NGC4594	Sa	9.8	240	$1.0(1.0, 0.7) \times 10^9$	s-12	1.57	5.0	-21.3	-24.2	-24.8	-25.4	5.1 ± 1.3	$2.0 \pm 0.5 \times 10^{11}$
NGC3608	E2	22.9	182	$1.9(1.0, 0.6) \times 10^8$	s-4	0.22	4.4	-19.9	-23.4	-24.0	-24.1	4.3 ± 1.1	$9.9 \pm 2.7 \times 10^{10}$
NGC3245	S0	20.9	205	$2.1(0.5, 0.5) \times 10^8$	g-13	0.21	4.2	-19.6	-22.4	-23.1	-23.3	1.3 ± 0.3	$3.9 \pm 1.0 \times 10^{10}$
NGC4291	E2	26.2	242	$3.1(0.8, 2.3) \times 10^8$	s-4	0.18	3.6	-19.6	-23.1	-23.8	-23.9	2.3 ± 0.6	$9.5 \pm 2.5 \times 10^{10}$
NGC3377	E5	11.2	145	$1.0(0.9, 0.1) \times 10^8$	s-4	0.38	3.6	-19.0	-22.7	-23.5	-23.6	5.4 ± 1.3	$7.8 \pm 2.1 \times 10^{10}$
NGC4473	E5	15.7	190	$1.1(0.4, 0.8) \times 10^8$	s-4	0.17	3.4	-19.9	-23.1	-23.6	-23.8	2.8 ± 0.7	$6.9 \pm 1.9 \times 10^{10}$
CygnusA	E	240	270	$2.9(0.7, 0.7) \times 10^9$	g-14	0.15	2.9	-21.9	-26.4	-26.9	-27.3	31 ± 8	$1.6 \pm 1.1 \times 10^{12}$
NGC4261	E2	31.6	315	$5.2(1.0, 1.1) \times 10^8$	g-15	0.15	2.9	-21.1	-24.6	-25.4	-25.6	6.5 ± 1.6	$4.5 \pm 1.2 \times 10^{11}$
NGC4564	E3	15.0	162	$5.6(0.3, 0.8) \times 10^7$	s-4	0.13	2.5	-18.9	-22.5	-23.3	-23.4	3.0 ± 0.7	$5.4 \pm 1.5 \times 10^{10}$
NGC4742	E4	15.5	90	$1.4(0.4, 0.5) \times 10^7$	s-16	0.10	2.0	-18.9	-22.1	-22.8	-23.0	2.0 ± 0.5	$1.1 \pm 0.3 \times 10^{10}$
NGC3379	E1	10.6	206	$1.0(0.6, 0.5) \times 10^8$	s-17	0.20	1.9	-19.9	-23.1	-23.7	-24.2	2.9 ± 0.7	$8.5 \pm 2.3 \times 10^{10}$
NGC1023	SB0	11.4	205	$4.4(0.5, 0.5) \times 10^7$	s-18	0.08	1.6	-18.4	-22.6	-23.3	-23.5	1.2 ± 0.3	$3.4 \pm 0.9 \times 10^{10}$
NGC5845	E3	25.9	234	$2.4(0.4, 1.4) \times 10^8$	s-4	0.15	1.4	-18.7	-22.0	-22.7	-23.0	0.50 ± 0.12	$1.9 \pm 0.5 \times 10^{10}$
NGC3384	S0	11.6	143	$1.6(0.1, 0.2) \times 10^7$	s-4	0.06	1.2	-19.0	-21.7	-22.3	-22.6	0.49 ± 0.12	$7.0 \pm 1.9 \times 10^9$
NGC6251	E2	107.0	290	$6.1(2.0, 2.1) \times 10^8$	g-19	0.06	1.2	-21.5	-25.4	-26.4	-26.6	11 ± 3	$6.7 \pm 1.8 \times 10^{11}$
Group 2*													
MilkyWay	SBbc	0.008	103	$4.1(0.6, 0.6) \times 10^6$	s-20	42.9	1714	-17.6	-22.0	-22.2	-22.3	0.70 ± 0.20	$5.2 \pm 2.5 \times 10^9$
M31	Sb	0.8	160	$4.5(4.0, 2.5) \times 10^7$	s-21	2.05	41	-19.0	-21.8	-22.5	-22.8	1.0 ± 0.3	$1.9 \pm 0.5 \times 10^{10}$
NGC1068	Sb	15.0	151	$8.3(0.3, 0.3) \times 10^6$	m-22	0.02	2.7	-18.8	-23.6	-24.7	-25.0	3.1 ± 0.8	$5.0 \pm 1.4 \times 10^{10}$
NGC4459	S0	16.1	186	$7.0(1.3, 1.3) \times 10^7$	g-11	0.11	2.2	-19.1	-23.9	-24.2	-24.5	15 ± 4	$3.6 \pm 1.0 \times 10^{11}$
NGC4596	SB0	27.9	152	$7.8(4.2, 3.3) \times 10^7$	g-11	0.11	2.1	-20.6	-23.0	-23.7	-23.8	1.6 ± 0.4	$2.6 \pm 0.7 \times 10^{10}$
NGC7457	S0	13.2	67	$3.5(1.1, 1.4) \times 10^6$	s-4	0.05	1.0	-17.7	-21.3	-22.0	-21.8	4.8 ± 3.5	$1.5 \pm 1.1 \times 10^{10}$
NGC4342	S0	11.4	225	$2.2(1.3, 0.8) \times 10^8$	s-23	0.34	0.8	-16.4	-20.1	-20.7	-20.7	0.29 ± 0.07	$1.0 \pm 0.3 \times 10^{10}$
NGC0821	E4	24.1	209	$3.7(2.4, 0.8) \times 10^7$	s-4	0.03	0.6	-20.4	-24.4	-24.9	-24.8	20 ± 5	$6.2 \pm 1.7 \times 10^{11}$
NGC2778	E2	22.9	175	$1.4(0.8, 0.9) \times 10^7$	s-4	0.02	0.4	-18.6	-22.0	-22.8	-23.0	3.0 ± 0.8	$6.5 \pm 1.7 \times 10^{10}$
NGC7052	E4	71.4	266	$4.0(2.8, 1.6) \times 10^8$	g-24	0.07	0.5	-21.7	-25.2	-25.9	-26.1	12 ± 3	$6.0 \pm 1.6 \times 10^{11}$

Note. — (1) Galaxy Name. (2) Morphological type from RC3. (3) Galaxy Distance in Mpc. (4) Stellar velocity dispersions from T02 and Kormendy & Gebhardt 2001 in units of km s^{-1} . All σ_* values have $\pm 5\%$ errors except for the Milky Way ($\pm 20 \text{ km s}^{-1}$), Cygnus A ($\pm 90 \text{ km s}^{-1}$, Thornton, Stockton, & Ridgway 1999) and NGC5252 ($\pm 27 \text{ km s}^{-1}$). (5) BH mass in units of M_{\odot} . '(+,-)' indicate the \pm errors. (6) Method of M_{BH} determination (g=gas kinematics, s=stellar dynamics, m=galaxy kinematics with maser spots) and references from where M_{BH} was obtained (if necessary it was rescaled to the distances in column 3). (7) Black hole sphere of influence, $R_{\text{BH}} = GM_{\text{BH}}/\sigma_*^2$, in arcseconds. (8) $N_{\text{res}} = 2R_{\text{BH}}/R_{\text{res}}$ where R_{res} is the spatial resolution of the observations (9) Absolute bulge B luminosity from T02 or extracted from the RC3 catalog (de Vaucouleurs et al. 1991). (10,11,12) Absolute J, H and K bulge magnitudes. Milky Way J and K values are taken from Dwek et al. (1995) while for M31 we have corrected the total galaxy magnitudes Malhotra et al. (1996) with the Simien & de Vaucouleurs (1986) disk-bulge average ratios; H values are interpolated. All M_{J} , M_{H} and M_{K} values have errors ± 0.1 mag except for the Milky Way ($\Delta M_{\text{J}} = 0.75$, $\Delta M_{\text{H}} = 0.75$, $\Delta M_{\text{K}} = 0.75$), M31 (0.4, 0.5, 0.4), Centaurus A (0.2, 0.3, 0.2), NGC 1068 (0.6, 0.6, 0.6) and NGC 7457 (0.6, 0.4, 0.4). (13) J band effective bulge radius in kpc. For the Milky Way we have taken the estimate by T02, while for M31 we have used that by Kormendy & Bender (1999). (14) Virial bulge mass in units of M_{\odot} .

* Though the Milky Way represents by far the best case for a BH, it has been placed in group 2 because existing measurements of the bulge near-IR luminosity are uncertain and because it is beyond the scope of this paper to estimate the luminosity of the Milky Way bulge from 2MASS data. This is also the case for M31. NGC 1068 is in group 2 because the BH mass estimate is not 'secure' in the sense that the maser spots are moving sub-keplerianly (Greenhill et al. 1996) and M_{BH} depends on the adopted disk model (Lodato & Bertin 2003). Also the complex morphology did not allow to obtain an accurate estimate of the bulge luminosity. In the cases of NGC 4459 and NGC 4596, the data do not allow a tight constraint on M_{BH} (Sarzi et al. 2001).

References. — 1) Hernstein et al. 1999; 2) Macchetto et al. 1997; 3) Emsellem, Dejonghe, & Bacon 1999; 4) Gebhardt et al. 2003; 5) Devereux et al. 2003; 6) average of Bower et al. 1998; Maciejewski & Binney 2001; 7) Verolme et al. 2002; 8) Marconi et al. 2001; 9) average of Verdoes Klein et al. 2000 and Cappellari et al. 2002; 10) Capetti et al. 2003; 11) Sarzi et al. 2001; 12) Kormendy 1988; 13) Barth et al. 2001; 14) Tadhunter et al. 2003; 15) Ferrarese et al. 1996; 16) T02; 17) Gebhardt et al. 2000; 18) Bower et al. 2001; 19) Ferrarese & Ford 1999; 20) Ghez et al. 2003; Schodel et al. 2002; 21) Tremaine 1995; Kormendy & Bender 1999; Bacon et al. 2001; 22) Lodato & Bertin 2003; Greenhill et al. 1996; 23) Cretton & van den Bosch 1999; 24) van der Marel & van den Bosch 1998

vations. Additional reasons for placing galaxies in Group 2 are given in Table 1.

3. IMAGE ANALYSIS

We have constructed a homogeneous set of NIR images of the galaxies presented in Table 1 (except for the Milky Way and

M31) by retrieving J, H, and K atlas images from the 2-Micron All Sky Survey (2MASS; <http://www.ipac.caltech.edu/2mass>). When a single atlas image contained only a portion of the galaxy, we also retrieved adjacent tiles and mosaicked the images after subtracting the sky background and rescaling for the different zero points. The 2MASS images are photometrically

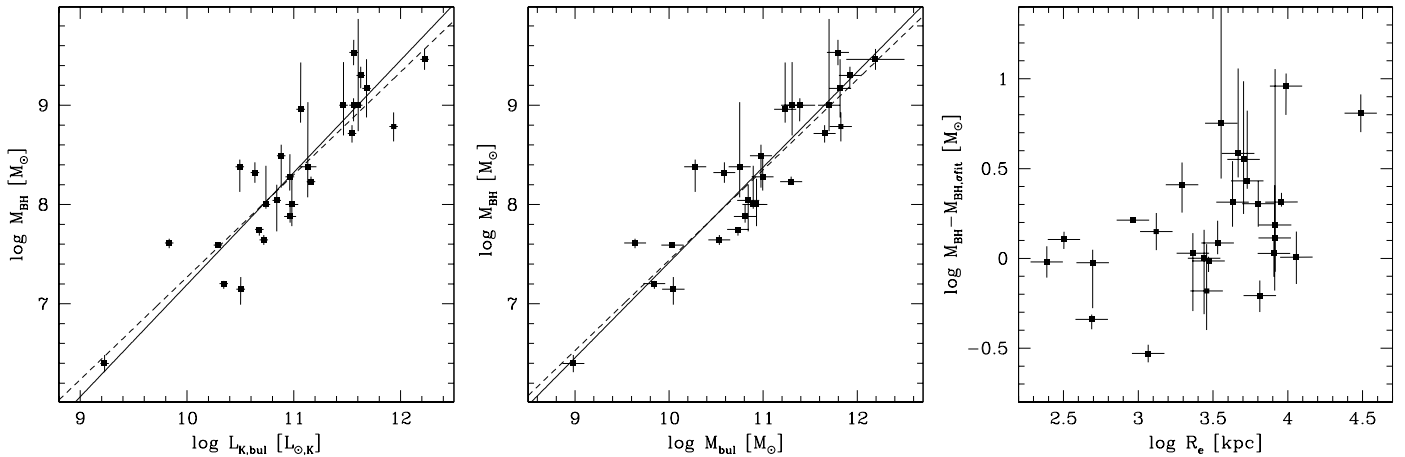


FIG. 1.— Left (a): M_{BH} vs $L_{\text{K,bul}}$ for the galaxies of Group 1. The solid lines are obtained with the bisector linear regression algorithm by Akritas & Bershady (1996), while the dashed lines are ordinary least square fits. Center (b): M_{BH} vs M_{bul} with the same notation as in the previous panel. Right (c): residuals of $M_{\text{BH}} - \sigma_e$ vs R_e , in which we use the $M_{\text{BH}} - \sigma_e$ regression by T02.

calibrated with a typical accuracy of a few percent. More details can be found in Hunt & Marconi (2003; hereafter Paper II).

We performed a 2D bulge/disk decomposition of the images using the program GALFIT (Peng et al. 2002) which is made publicly available by the authors. This code allows the fitting of several components with different functional shapes (e.g., generalized exponential (Sersic) and simple exponential laws); the best fit parameters are determined by minimizing χ^2 . More details on GALFIT can be found in Peng et al. (2002). We fit separately the J, H and K images. Each fit was started by fitting a single Sersic component and constant background. When necessary (e.g., for spiral galaxies), an additional component (usually an exponential disk) was added. In many cases these initial fits left large residuals and we thus increased the number of components (see also Peng et al. 2002). The fits are described in detail in Paper II. In Table 1 we present the J, H and K bulge magnitudes, effective bulge radii R_e in the J band, and their uncertainties. The J, H and K magnitudes were corrected for Galactic extinction using the data by Schlegel, Finkbeiner, & Davis (1998). We used the J band to determine R_e because the images tend to be flatter, and thus the background is better determined.

4. RESULTS AND DISCUSSION

In Fig. 1 we plot, from left to right, M_{BH} vs $L_{\text{K,bul}}$, M_{BH} vs M_{bul} , and the residuals of $M_{\text{BH}} - \sigma_e$ vs R_e (based on the fit from T02). Only Group 1 galaxies are shown. M_{bul} is the virial bulge mass given by $kR_e\sigma_e^2/G$; if bulges behave as isothermal spheres, $k = 8/3$. However, comparing our virial estimates M_{bul} with those M_{dyn} , obtained from dynamical modeling (Magorrian et al. 1998; Gebhardt et al. 2003), shows that M_{bul} and M_{dyn} are well correlated ($r = 0.88$); setting $k = 3$ (rather than $8/3$) gives an average ratio of unity. Therefore, we have used $k = 3$ in the above formula. Considering the uncertainties of both mass estimates, the scatter of the ratio $M_{\text{bul}}/M_{\text{dyn}}$ is 0.21 dex. We fit the data with the bisector linear regression from Akritas & Bershady (1996) which allows for uncertainties on both variables and intrinsic dispersion. The FITEXY routine (Press et al. 1992) used by T02 gives consistent results (see Fig. 1). Fit results of M_{BH} vs galaxy properties for Group 1 and the combined samples are summarized in Table 2. The intrinsic dispersion of the residuals (*rms*) has been estimated with

a maximum likelihood method assuming normally-distributed values. Inspection of Fig. 1 and Table 2 show that $L_{\text{K,bul}}$ and M_{bul} correlate well with the BH mass. The correlation between M_{BH} and M_{bul} is equivalent to that between the radius of the BH sphere of influence $R_{\text{BH}} (= GM_{\text{BH}}/\sigma_e^2)$ and R_e .

4.1. Intrinsic Dispersion of the Correlations

To compare the scatter of $M_{\text{BH}} - L_{\text{bul}}$ for different wavebands, we have also analyzed the B-band bulge luminosities for our sample. The upper limit of the intrinsic dispersion of the $M_{\text{BH}} - L_{\text{bul}}$ correlations goes from ~ 0.5 dex in $\log M_{\text{BH}}$ when considering all galaxies, to ~ 0.3 when considering only those of Group 1. Hence, for galaxies with reliable M_{BH} and L_{bul} , the scatter of $M_{\text{BH}} - L_{\text{bul}}$ correlations is ~ 0.3 , *independently of the spectral band used (B or JHK)*, comparable to that of $M_{\text{BH}} - \sigma_e$. This scatter would be smaller if measurement errors are underestimated. McLure & Dunlop (2002) and Erwin et al. (2003) reached a similar conclusion using R-band L_{bul} but on smaller samples. The correlation between R-band bulge light concentration and M_{BH} has a comparable scatter (Graham et al. 2001).

Since $M_{\text{BH}} - L_{\text{B,bul}}$ and $M_{\text{BH}} - L_{\text{NIR,bul}}$ have comparable dispersions, the rough bulge/disk decomposition (§1), the larger reddening and stellar population effects do not apparently compromise the correlation. Most of the galaxies in the sample are early types, and thus may be less sensitive to the above effects. However, the scatter in the $M_{\text{BH}} - L_{\text{bul}}$ correlations does not decrease significantly when considering only elliptical galaxies.

The correlation between M_{BH} and M_{bul} has a slightly lower dispersion (0.25 versus 0.3) than $M_{\text{BH}} - L_{\text{bul}}$. If the scatter of $M_{\text{bul}} - M_{\text{dyn}}$ (0.21 dex) is an indication of the additional uncertainties on our virial estimates, then the intrinsic scatter of $M_{\text{BH}} - M_{\text{bul}}$ drops to ~ 0.15 dex. Judging from the present data where only secure M_{BH} and L_{bul} are included, σ_e , M_{bul} , $L_{\text{B,bul}}$ and $L_{\text{NIR,bul}}$ provide equally good M_{BH} estimates to within a factor of ~ 2 .

4.2. Correlation slopes

All the slopes are roughly unity, but those of $M_{\text{BH}} - L_{\text{bul}}$ are systematically larger than that of $M_{\text{BH}} - M_{\text{bul}}$. This is expected if L_{bul} correlates with M_{BH} because of its dependence on M_{bul} through the stellar M/L ratio. From our $M_{\text{bul}} - L_{\text{bul}}$ relation, we find that $\log \Upsilon_K = 0.18 \log L_{\text{K,bul}} - 2.1$; the weak dependence of

TABLE 2
FIT RESULTS ($\log M_{\text{BH}} = a + bX$).

X	Group 1 Galaxies			All Galaxies		
	a	b	rms	a	b	rms
$\log L_{\text{B,bul}} - 10.0$	8.18 ± 0.08	1.19 ± 0.12	0.32	8.07 ± 0.09	1.26 ± 0.13	0.48
$\log L_{\text{J,bul}} - 10.7$	8.26 ± 0.07	1.14 ± 0.12	0.33	8.10 ± 0.10	1.24 ± 0.15	0.53
$\log L_{\text{H,bul}} - 10.8$	8.19 ± 0.07	1.16 ± 0.12	0.33	8.04 ± 0.10	1.25 ± 0.15	0.52
$\log L_{\text{K,bul}} - 10.9$	8.21 ± 0.07	1.13 ± 0.12	0.31	8.08 ± 0.10	1.21 ± 0.13	0.51
$\log M_{\text{bul}} - 10.9$	8.28 ± 0.06	0.96 ± 0.07	0.25	8.12 ± 0.09	1.06 ± 0.10	0.49

Υ on L fully accounts for the different slopes of $M_{\text{BH}}-L_{\text{K,bul}}$ and $M_{\text{BH}}-M_{\text{bul}}$, and the same applies to the J and H bands.

All correlations are thus consistent with a direct proportionality between M_{BH} and bulge mass. This contrasts with previous claims of a non-linearity of the $M_{\text{BH}}-M_{\text{bul}}$ relation (Laor 2001) but is in agreement with McLure & Dunlop (2002). A partial correlation analysis of $\log M_{\text{BH}}$ (variable x_1), $\log \sigma_e$ (x_2), and $\log R_e$ (x_3) shows that M_{BH} is *separately* significantly correlated both with σ_e and R_e . The Pearson partial correlation coefficients, in which the known dependence of σ_e and R_e is eliminated, are $r_{12} = 0.83$, $r_{13} = 0.65$, with a significance of $> 99.9\%$. This is shown graphically in Fig. 1c, where the residuals of the T02 $M_{\text{BH}}-\sigma_e$ correlation are plotted against R_e ; there is a weak, but significant, correlation of these residuals with R_e . Consequently, when galaxy structural parameters are measured carefully from 2D image analysis, the additional, weaker, dependence of M_{BH} on R_e is uncovered. Thus, a combination of both σ_e and R_e is necessary to drive the correlations between M_{BH} and other bulge properties. This *fundamental plane* of

black holes will be further investigated elsewhere.

The average $\log M_{\text{BH}}/M_{\text{bul}}$ can be estimated assuming a log-normal distribution with normally distributed observational errors. With maximum likelihood we find $\langle \log M_{\text{BH}}/M_{\text{bul}} \rangle = -2.63$ with an intrinsic dispersion of 0.27 dex (-2.79 and 0.49 dex for all galaxies). Adopting the method of Merritt & Ferrarese (2001), we find $\langle \log M_{\text{BH}}/M_{\text{bul}} \rangle = -2.81$ and $rms = 0.36$ (-2.86 and 0.44 for all galaxies) consistently with their result of -2.9 and 0.45 dex (see also McLure & Dunlop 2002).

We thank A. Capetti, E. Emsellem, W. Maciejewski, C. Norman, and E. Oliva for useful discussions. This paper was partially supported by ASI (I/R/112/01 and I/R/048/02) and MIUR (Cofin01-02-02). This publication uses the LEDA database, the NASA/IPAC Extragalactic Database operated by JPL, CalTech, under contract with NASA, and data products from 2MASS, a joint project of the University of Massachusetts and the IPAC/CalTech, funded by NASA and NSF.

REFERENCES

- Akritas, M. G. & Bershad, M. A. 1996, ApJ, 470, 706
 Aller, M. C. & Richstone, D. 2002, AJ, 124, 3035
 Bacon, R., Emsellem, E., Combes, F. et al. 2001, A&A, 371, 409
 Barth, A. J., Sarzi, M., Rix, H. et al. 2001, ApJ, 555, 685
 Bower, G. A. et al. 2001, ApJ, 550, 75
 Bower, G. A., et al. 1998, ApJ, 492, L111
 Cappellari, M., Verolme, E. K., van der Marel, R. P. et al. 2002, ApJ, 578, 787
 Capetti, A., Macchetto, D., Axon, D. J., & Marconi, A. 2003, in preparation
 de Vaucouleurs, G. et al. 1991, Third reference catalogue of Bright galaxies, New York: Springer-Verlag (RC3)
 Cretton, N. & van den Bosch, F. C. 1999, ApJ, 514, 704
 Devereux, N. A., Ford, H. C., Tsvetanov, Z., & Jacoby, G. 2003, AJ, 125, 1226
 Dwek, E. et al. 1995, ApJ, 445, 716
 Emsellem, E., Dejonghe, H., & Bacon, R. 1999, MNRAS, 303, 495
 Erwin, P., Graham, A. W., & Caon, N. 2003, Carnegie Observatories Astrophysics Series, Vol. 1, ed. L. C. Ho (astro-ph/0212335)
 Ferrarese, L. & Ford, H. C. 1999, ApJ, 515, 583
 Ferrarese, L., Ford, H. C., & Jaffe, W. 1996, ApJ, 470, 444
 Ferrarese, L. & Merritt, D. 2000, ApJ, 539, L9
 Ferrarese, L. 2002, in "Current High-Energy Emission around Black Holes", Eds. C.-H. Lee & H.-Y. Chang. Singapore: World Scientific, p. 3
 Gavazzi, G. 1993, ApJ, 419, 469
 Gebhardt, K. et al. 2000, ApJ, 539, L13
 Gebhardt, K. et al. 2000, AJ, 119, 1157
 Gebhardt, K. et al. 2003, ApJ, 583, 92
 Ghez, A. M. et al. 2003, ApJ Letters, in press (astro-ph/0302299)
 Graham, A. W., Erwin, P., Caon, N., & Trujillo, I. 2001, ApJ, 563, L11
 Greenhill, L. J. et al. 1996, ApJ, 472, L21
 Herrnstein, J. R. et al. 1999, Nature, 400, 539
 Hunt, L. K., & Marconi, A. 2003, in preparation (Paper II)
 Kormendy, J., & Richstone, D. 1995, ARA&A, 33, 581
 Kormendy, J. 1988, ApJ, 335, 40
 Kormendy, J. & Bender, R. 1999, ApJ, 522, 772
 Kormendy, J., & Gebhardt, K. 2001, in 20th Texas Symposium on Relativistic Astrophysics, eds. J. C. Wheeler and H. Martel (Melville, NY: AIP), 363
 Laor, A. 2001, ApJ, 553, 677
 Lodato, G. & Bertin, G. 2003, A&A, 398, 517
 Macchetto, F., Marconi, A., Axon, D. J. et al. 1997, ApJ, 489, 579
 Maciejewski, W. & Binney, J. 2001, MNRAS, 323, 831
 Magorrian, J. et al. 1998, AJ, 115, 2285
 Malhotra, S., Spergel, D. N., Rhoads, J. E., & Li, J. 1996, ApJ, 473, 687
 Marconi, A., Capetti, A., Axon, D. J. et al. 2001, ApJ, 549, 915
 Marconi, A., & Salvati, M. 2002, PASP Conf. Series 258, 217 (astro-ph/0110698)
 McLure, R. J., & Dunlop, J. S. 2002, MNRAS, 331, 795
 Merritt, D. & Ferrarese, L. 2001, MNRAS, 320, L30
 Merritt, D. & Ferrarese, L. 2001, in The Central Kiloparsec of Starbursts and AGN, eds. J. H. Knapen et al. (San Francisco: ASP), 335
 Peng, C. Y., Ho, L. C., Impey, C. D., & Rix, H.-W. 2002, AJ, 124, 266
 Press, W. H. et al. 1992, Numerical Recipes in C, (Cambridge: University Press), 2nd edition.
 Sarzi, M., Rix, H., Shields, J. C. et al. 2001, ApJ, 550, 65
 Schodel, R., Ott, T., Genzel, R. et al. 2002, Nature, 419, 694
 Simien, F., & de Vaucouleurs, G. 1986, ApJ, 302, 564
 Soltan, A. 1982, MNRAS, 200, 115
 Schlegel, D. J., Finkbeiner, D. P., & Davis, M. 1998, ApJ, 500, 525
 Tadhunter, C., Marconi A., Axon, D. J. et al. 2003, MNRAS, in press (astro-ph/0302513)
 Thornton, R. J., Stockton, A., & Ridgway, S. E. 1999, AJ, 118, 1461
 Tonry, J., Blakeslee, J., Ajhar, E., & Dressler, A. 2000, ApJ, 530, 625
 Tremaine, S. 1995, AJ, 110, 628
 Tremaine, S. et al. 2002, ApJ, 574, 740
 van der Marel, R. P., & van den Bosch, F. C. 1998, AJ, 116, 2220
 Verdoes Kleijn, G. A. et al. 2000, AJ, 120, 1221
 Verolme, E. K. et al. 2002, MNRAS, 335, 517
 Yu, Q. & Tremaine, S. 2002, MNRAS, 335, 965